Electrification hazard of turbulent pipe flow: Theoretical approach and numerical simulation

Xu Diao, Juncheng Jiang, Lei Ni, Ahmed Mebarki, Guodong Shen

Version of Record: https://www.sciencedirect.com/science/article/pii/S0957582021007187
Manuscript_cace74c159c33e5eca6d28e17be03f20

Electrification hazard of turbulent pipe flow: theoretical approach and numerical simulation

Xu Diao[a,c], Juncheng Jiang[a,b*], Lei Ni[a], Ahmed Mebarki[c,a **1],Guodong Shen[a]

[a] *Jiangsu Key Laboratory of Hazardous Chemicals Safety and Control, Nanjing Tech University, Nanjing, 211816, Jiangsu, China;*

[b] *School of Environmental and Safety Engineering, Changzhou University, Changzhou, 213164, Jiangsu, China;*

[c] *University Gustave Eiffel, UPEC, CNRS, Laboratory Multi Scale and Simulation (MSME: Univ. Gustave Eiffel, UPEC, CNRS/UMR 8208), 5 blvd Descartes, 77454 Marne-La-Vallee, France*

Abstract: The present paper deals with electrostatic characteristics, i.e., space charge density and electrostatic potential under turbulent flow in pipes with and without leakage. This paper considers the charge conservation equation and proposes theoretical models able to calculate the space charge density of intact and leak pipes. The distributions of the space charge density and electrostatic potential are investigated through numerical simulation. For the case study used for validation purposes, the space charge density obtained by numerical simulations is compared with the experimental results. The results show that the proposed model is capable of calculating adequately the distribution of the space charge density in pipes. The effects of flow velocity and pipe diameter on the electrostatic characteristics of intact and leak pipes are then investigated. The results show that, for intact pipes, the maximum electrostatic potential appears in the central area of the pipe and increases slowly with the increase of the velocity, while the maximum potential decreases with the increase of the pipe diameter. For leak pipes, the maximum potential takes place at the leak aperture, and increases with the increase of flow velocity and pipe diameter. In order to reduce the possibility of electrostatic discharge, the flow velocity ought to be controlled below 2.5 m/s, and the pipes with smaller diameter shall be used as far as possible when meeting the requirement for use.

Graphic Abstract：

* Corresponding author at: Jiangsu Key Laboratory of Hazardous Chemicals Safety and Control, Nanjing Tech University, Nanjing, 211816, Jiangsu, China; E-mail addresses: jcjiang_njtech@163.com. (J C. Jiang)
** Corresponding author at: University Gustave Eiffel, UPEC, CNRS, Laboratory Multi Scale Modeling and Simulation (MSME / UMR 8208 CNRS), 5 Bd Descartes, 77454, Marne-La-Vallee, France; E-mail addresses: Ahmed.Mebarki@univ-paris-est.fr. (A.Mebarki)
[1] Guest Professor at Nanjing Tech University, within “High-Level Foreign Talents” grant.

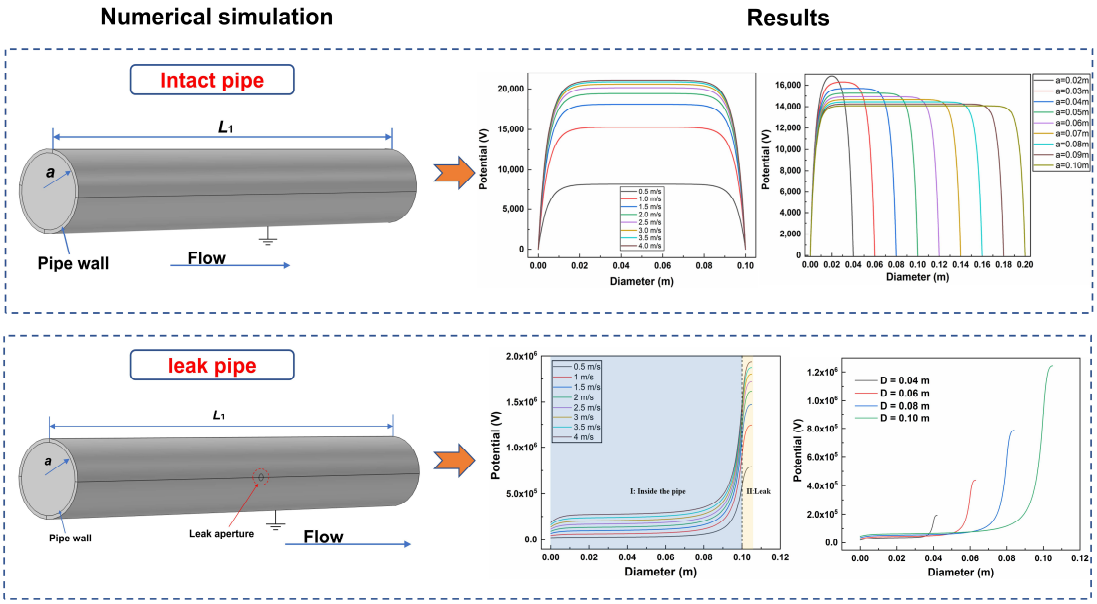

Keywords: Flow electrification models; Numerical simulation; Space charge density; Electrostatic potential; Leak pipe.

1. Introduction

Chemical industry and oil refining are typical process industries, and pipelines play an increasingly important role in the transportation of petroleum and chemical products. When dielectric liquids, such as lighten oil, are in contact with pipe wall, physicochemical process generates an electrical double layer (EDL) (Pavey, 2004; Zheng et al., 2013). The additives or impurities contained in the liquid may dissociate into positive and negative ions, thus the EDL is constituted of two different zones with opposite signs, one sign inside the solid surface and the opposite sign inside the liquid (Moreau et al., 2001), as shown in Fig. 1. The thickness of EDL is assimilated to the Debye length, which is an inherent property of the liquid. The EDL of the flowing dielectric liquid can generate static electricity so that when the cumulated electrostatic charges reach a certain threshold, they will discharge in the form of a spark and result in a fire if a flammable vapor reaches the flammability limits (Giles, 2003). Especially, when a pipe containing flammable liquid leaks, the leaking liquid volatilizes and forms a flammable atmosphere. Although static electricity is not the most common cause of fires and explosions in the process industries, it is, however, a very important one (Pavey, 2004). Chou et al. (2015) investigated an explosion accident caused by static electricity in a propylene plant. The explosion was generated by the ignition caused when the high volume of leaked volatile acetone in the air made contact with the static electric spark. Therefore, the investigation of electrostatic characteristics of pipes is of great importance for the pipeline safety and the process industries.

Flow electrification of pipes has been studied for over 50 years. In early times, limited by computation capacities, researchers were more focused on theoretical models. Boumans (1957)

conducted theoretical and experimental studies on the streaming current in metal capillaries. Gavis and Kosman investigated theoretically the charge generation phenomenon, and proposed the equations corresponding to the streaming currents in low conductivity liquids under turbulent-flow conditions (Gavis, 1964; Gavis and Koszman, 1961; Koszman and Gavis, 1962). From the 1970s, Touchard (1978) studied the streaming current for both laminar and turbulent flow, and the experimental values corresponded to the theoretical values. He also gave the expressions and figures of the space charge density under laminar flow in a circular pipeline (Touchard et al., 1996). However, the space charge density at the interface needs to be known in advance. Abedian and Sonin (1982) proposed an explicit analytic form for convection current in the pipe, valid for all turbulent Reynolds numbers and all fluid conductivities (typical liquid hydrocarbons). Then they compared the proposed expressions with available experimental data. The results showed that theory is capable of calculating the streaming current of long, smooth-walled pipes under turbulent flow conditions (Abedian and Sonin, 1986). Wang and Meng (2009) investigated the effect of temperature on electrification and defined the boundary condition at the pipe wall, applicable to all oil conductivities in order to calculate the streaming current in oil. Zdanowski (2020) analyzed the influence of flow speed, temperature, and pipe material on the values of the electrification current and space charge density. In recent years, due to the increasing computational capacities, numerical simulation became an important way to verify theoretical models. El-Adawy et al. (2011) presented a numerical simulation of the EDL development process in the case of a liquid containing additives or impurities. The simulation results showed that the model for the general tendency of the EDL development agrees with the experimental results. Huang et al., (2016) used COMSOL software to estimate the impact of space charge density on the electric field distribution in the oil/paper insulation. Dai et al. (2018) proposed a simulation method to estimate the streaming current under DC voltage based on the bipolar charge transport model.

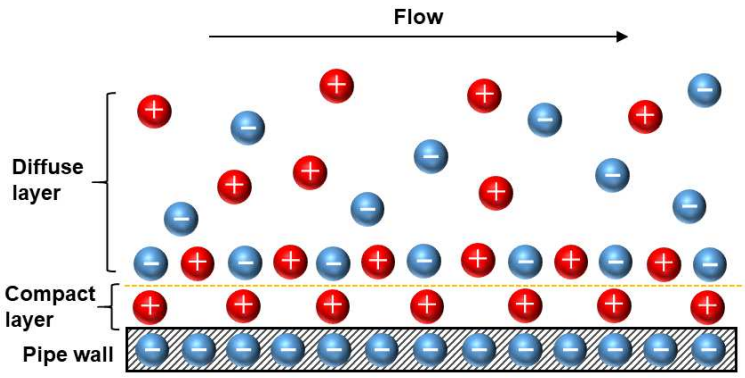

Fig.1. Schematic of the electrical double layer.

The whole models appear to be suitable for intact pipes. In fact, as for an intact pipe, even if the space charge density is large, the dielectric liquid may not show a large electrostatic potential due to its large capacitance (Walmsley, 2012). What's more, there is no air in the flowing pipe, so that the possibility of electrostatic discharge can be negligible. However, according to the statistical analysis of fires and explosions attributed to electrostatics done by Ohsawa (2011), liquid discharge by leakage accounted for 20.6% of the leading causes.

Furthermore, over 70% of the flammable atmospheres examined were formed by vapors, especially in a leak pipe. On the one hand, the flammable vapor emitted by the leaked liquid may reach the explosion limit. On the other hand, when the leaked dielectric field strength reaches a certain degree, such as exceeding the breakdown field strength of liquid vapor, it will increase the possibility of electrostatic discharge and increase the possibility of electrostatic ignition accident. In 2013, a crude oil vapor explosion accident occurred in Qingdao, China in 2013 due to the crude oil leaking from an underground pipeline into the urban storm drain. The volatilized oil vapors encountered with the spark and then were ignited, resulting in 62 fatalities and 136 injuries (Zhu et al., 2015).

Therefore, the present study proposes theoretical models for space charge density and potential in intact and leak pipes under turbulent flow. Their validation is investigated through simulations implemented and run by the commercial software COMSOL Multiphysics® (2018). The effects of the flow velocity and the pipe diameter on the space charge density and electrostatic potential of both intact and leak pips are studied.

2. Theory

2.1. Governing equations for the intact pipes

2.1.1. Equations of space charge density

The mechanism of flow electrification of dielectric liquid is complex and many factors affect the electrification. The mathematical model needs to be built under some assumptions and simplifications.

Hypothesis 1: The pipe flow is considered as the isothermal flow.

Hypothesis 2: The fluid is supposed incompressible.

Hypothesis 3: The charge density generated by the flow is low enough to have a negligible effect on the liquid conductivity and the conductivity is evenly distributed in the flow field.

The transport of charges is influenced in combination with diffusion, conduction, and convection (Leblanc et al., 2017). Thus, the current density $\mathbf{j}$ is a sum of current densities arising from these mechanisms:

$$\mathbf{j} = \mathbf{j}_{\text{diff}} + \mathbf{j}_{\text{cond}} + \mathbf{j}_{\text{conv}} = -D\nabla q + \sigma\mathbf{E} + q\mathbf{u} \tag{1}$$

where D is the diffusion coefficient; q is the space charge density; σ is the liquid conductivity; $\mathbf{E}$ is the electric field; $\mathbf{u}$ is the velocity field.

The charge conservation equation is described as:

$$\frac{\partial q}{\partial t} + \nabla\cdot\mathbf{j} = 0 \tag{2}$$

where t is the time. By substituting Eq. (1) into Eq. (2), the charge conservation equation at steady state can be written as:

$$\frac{\partial q}{\partial t} + \nabla\cdot(-D\nabla q + \sigma\mathbf{E} + q\mathbf{u}) = 0 \tag{3}$$

It can be derived as:

$$\frac{\partial q}{\partial t} - \nabla\cdot(D\nabla q) + \sigma\nabla\cdot\mathbf{E} + \nabla\cdot(q\mathbf{u}) = 0 \tag{4}$$

According to Gauss's law, the relationship between the electric field and charge density is:

$$\nabla\cdot\mathbf{E} = q/\varepsilon \tag{5}$$

where $\varepsilon = \varepsilon_r \times \varepsilon_0$ is the permittivity of the liquid, in which ε_r is the relative permittivity and $\varepsilon_0 = 8.854\times10^{-12}$ F/m is the vacuum permittivity. By substituting Eq. (5) into Eq. (4), the charge conservation equation becomes:

$$\frac{\partial q}{\partial t} - \nabla\cdot(D\nabla q) + \frac{\sigma q}{\varepsilon} + \nabla\cdot(q\mathbf{u}) = 0 \tag{6}$$

The last term in Eq. (6) can be expanded as:

$$\nabla\cdot(q\mathbf{u}) = \nabla q\cdot\mathbf{u} + q(\nabla\cdot\mathbf{u}) \tag{7}$$

Provided that the fluid in the pipe is imcompressible,

$$\nabla\cdot\mathbf{u} = 0 \tag{8}$$

the Eq. (6) takes the following form:

$$\frac{\partial q}{\partial t} - \nabla\cdot(D\nabla q) + \frac{\sigma q}{\varepsilon} + \nabla q\cdot\mathbf{u} = 0 \tag{9}$$

In turbulent flow, the influence of turbulence cannot be ignored. Thus, the diffusion coefficient consists of two parts, namely the molecular diffusion coefficient D_m in the laminar sublayer near the pipe wall and the turbulent diffusion coefficient D_t in the turbulent zone. Equation (9) can be represented as:

$$\frac{\partial q}{\partial t} - \nabla\cdot[(D_\mathrm{m}+D_t)\nabla q] + \frac{\sigma q}{\varepsilon} + \nabla q\cdot\mathbf{u} = 0 \tag{10}$$

The electrical potential ϕ of the pipe can be obtained by the Poisson's equation:

$$\nabla^2\phi = -q/\varepsilon \tag{11}$$

In Eq. (10), $\mathbf{u}$ is the velocity field vector. In order to solve this equation, a coordinate system of the pipeline is established, as shown in Fig. 2 to convert the velocity vector into a scalar. In turbulent flow, axial flow is dominant over radial flow, so that it can be assumed that the radial convection current is negligible ($\bar{u}_r\partial q/\partial r \approx 0$) compared with axial convection current (Zmarzly, 2013). Thus, the last term in Eq. (10) becomes $\bar{u}_x\partial q/\partial x$.

If there is no flow in the pipe, no electrostatic charge will be generated. Electrification occurs when the dielectric liquid flows through the pipe. This study is focused on the electrification phenomenon under steady state. In this case, the charge distribution is constant over time. Thus, the component $\partial q/\partial t$ is negligible in Eq. (10). Finally, the charge conservation equation in steady-state for the incompressible flow becomes:

$$-\nabla\cdot[r(D_\mathrm{m} + D_\mathrm{t})\nabla q] + \frac{\sigma q}{\varepsilon} + \bar{u}_x\frac{\partial q}{\partial x} = 0 \tag{12}$$

where $\bar{u}_x$ is the time-averaged axial velocity.

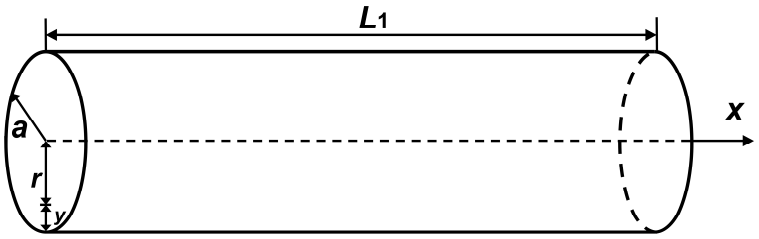

Fig. 2. The coordinate system of the pipeline.

2.1.2. Boundary conditions

Assuming that an infinite pipeline with the length of L has formed a fully developed flow, in order to solve the above differential equations, spatial boundary conditions of the space charge density are needed at the entrance, downstream and the pipe axis:

- (1) the space charge density at the entrance is known and can be assumed as being: $q|_{x=0} = 0$;
- (2) for the fully developed flow, the charge density at the end of the pipe is steady, $\partial q/\partial x|_{x=L} = 0$;
- (3) since the pipe is symmetrical, the charge distribution in the pipe axis is seen as: $\partial q/\partial r|_{r=0} = 0$.

In this study, a pipe section with the length of L_1 is studied, as shown in Fig. 2. It is a part at the end of an infinite pipeline with the length of L, which has fully developed.

However, the boundary condition of space charge density at the wall-liquid interface is difficult to quantify. When the liquid begins to flow in the pipe, the initial charge balance state will be destroyed, resulting in concentration gradient. Assuming that negative ions are depleted near the surface, as shown in Fig. 1, the negative ions in the liquid diffuse to the surface at a rate as rapid as the discharge rate. In this case, the surface current flux caused by the concentration polarization can be written as (Gavis and Koszman 1961):

$$j_s = -\frac{D_m F}{n_+ d}(C_{-o} - C_s) \tag{13}$$

where j_s is the streaming current at the surface; F is the Faraday's constant; C_{-o} is the concentration of the negative ions in the liquid bulk; C_s is the concentration at the surface; n_+ is the transference number of the positive ions; d is the diffuse layer thickness. The concentrations C_{-o} and C_s are considered to be constant (Koszman and Gavis, 1962).

The other polarization effect is the progressive build-up in the liquid of excess positive charges, resulting in potential difference. This effect is added and expressed as:

$$j_s = -\frac{D_m F}{n_+ d}(C_{-o} - C_s) - \left.\frac{\partial \phi}{\partial r}\right|_{r=a} \tag{14}$$

where a is the pipe radius.

According to the research done by Nelson et al. (2003), the streaming current near the wall j_w is written as:

$$j_w = \sigma \bar{E} - D_m \nabla q = -\sigma \left.\frac{\partial \phi}{\partial r}\right|_{r=a} - D_m \left.\frac{\partial q}{\partial r}\right|_{r=a} \tag{15}$$

where $\bar{E}$ is the average electric field near the wall.

Comparison of Eqs. (14) and (15) shows that

$$\left.\frac{\partial q}{\partial r}\right|_{r=a} = \frac{F(C_{-o}-C_s)}{n_+ d} = \text{Constant} \tag{16}$$

Equation (16) shows that the charge density gradient at the surface is related to the properties of the liquid, the pipe wall and their physicochemical combinations. Thus, the values of the parameters in Eq. (16) are hard to evaluate. Wang gave another expression in which the current density depends on the ion concentration, the flow velocity, and other unknown factors (Wang and Meng, 2009).

$$\left.\frac{\partial q}{\partial r}\right|_{r=a} = C_{-o} A_t (U_m)^n \tag{17}$$

where A_t and n are the introduced constants and their values are determined by experimental data; U_m is the average velocity in the pipe cross-section; Assuming that the conductivity of the liquid is related to the negative ions from the EDL, C_{-o} is then defined as:

$$C_{-o} = \frac{\sigma}{2F\mu} \tag{18}$$

where μ is the average mobility of the positive and negative ions.

Since the mobility of the ions in the liquid is hard to measure, the Eq. (18) is derived as the following expression based on the electrical mobility equation of the Einstein's relation ($D=kT\mu/e_0$):

$$C_{-o} = \frac{\sigma kT}{2FDe_0} \tag{19}$$

where k is the Boltzmann constant; T is the absolute temperature; e_0 is the electrical charge of a particle.

Therefore, the combination of Eq. (17) and (19) gives the boundary condition of charge density gradient at the interface as:

$$\left.\frac{\partial q}{\partial r}\right|_{r=a} = \frac{\sigma kT A_t (U_m)^n}{2FDe_0} = C \tag{20}$$

2.1.3. Solutions the space charge density

The differential equations solution request prior knowledge of the turbulent diffusivity D_t and the axial velocity u_x. The velocity distribution is approximately linear in the laminar sublayer, and logarithmic in the core region of turbulence. Furthermore, with the increase of the Reynolds number (Re), the intensity of turbulence increases, so that the thickness of the laminar sublayer becomes thinner and the velocity in the turbulent core area becomes approximately constant.

As for the pipe section studied in this paper, turbulences are already fully developed. Thus the flow is steady in this pipe section and the space charge distribution no longer changes with the axial distance x, but only depends on the pipe radius. With such assumption the convection component can be ignored $(\bar{u}_x \partial q/\partial x = 0)$ and then Eq. (10) is reduced as:

$$\frac{1}{r}\frac{\partial}{\partial r}[r(D_m + D_t)\frac{\partial q}{\partial r}] = \frac{\sigma q}{\varepsilon} \tag{21}$$

In the laminar sublayer, the influence of turbulence is considerably small so that the turbulent diffusion coefficient D_t can be neglected when compared with the molecular diffusion

coefficient D_m.

Thus, the Eq. (21) becomes:

$$\frac{1}{r}\frac{\partial}{\partial r}(rD_m\ \frac{\partial q}{\partial r}) = \frac{\sigma q}{\varepsilon} \tag{22}$$

Since this thin area is located near the wall, it is convenient to use a Cartesian coordinate system to solve Eq. (22). Assuming $y = a\text{-}r$, as shown in Fig. 2, the Eq. (22) is transformed to:

$$\frac{\partial^2 q_1}{\partial y^2} = \frac{q_1}{\lambda^2} \tag{23}$$

where q_1 is the space charge density in laminar sublayer; $\lambda = \sqrt{D_m\varepsilon/\sigma}$ is the Debye length, which represents the distance at which the charged layer permeates from the wall into the liquid in the laminar sublayer.

In turbulent region, the turbulent diffusion coefficient D_t plays a major role, while the molecular diffusion coefficient D_m is negligible. The turbulent diffusion coefficient is obtained by (Wang and Meng, 2010):

$$D_t = 22.19v \tag{24}$$

where v is the kinematic viscosity of the dielectric liquid.

Thus, Eq. (21) is simplified as:

$$\frac{1}{r}\frac{\partial}{\partial r}(rD_t\ \frac{\partial q_2}{\partial r}) = \frac{\sigma q_2}{\varepsilon} \tag{25}$$

Equation (25) can be derived as the form of the modified Bessel equation:

$$b^2\frac{\partial^2 q_2}{\partial z^2} + b\frac{\partial q_2}{\partial z} - b^2 q_2 = 0 \tag{26}$$

where q_2 is the space charge density in turbulent region; the variable $b = r/\lambda_t$, in which $\lambda_t = \sqrt{D_t\varepsilon/\sigma}$ is the turbulent Debye length.

The general solution of Eq. (23) and (26) is

$$\begin{cases} q_1 = C_1\cosh(y/\lambda) + C_2\sinh(y/\lambda) \\ q_2 = C_3 I_0(r/\lambda_t) + C_4 K_0(r/\lambda_t) \end{cases} \tag{27}$$

where C_1~C_4 are the coefficients that need to be determined using boundary conditions; $I_0()$ and $K_0()$ are the zero-order modified Bessel functions of the first and second kind, respectively.

The space charge density and the electric field at the interface between the laminar sublayer and turbulent zone should meet continuity conditions.

$$\begin{cases} q_1 = q_2, \quad y = \delta \\ D_m\frac{\partial q_1}{\partial y} = D_t\frac{\partial q_2}{\partial r}, \quad y = \delta \end{cases} \tag{28}$$

where δ is the thickness of the laminar sublayer, which can be estimated for high Schmidt numbers:

$$\delta = \kappa v(\tau_w/\rho)^{-1/2}S^{-1/m} \tag{29}$$

where τ_w is the shear stress at the wall; ρ is the liquid density; S is the Schmidt number ($S = v/D_m$); κ and m are the empirical coefficients and previous researches implied $m = 3$ and $\kappa = 11.7\text{–}13.5$ (Abedian and Sonin, 1986) so that $m = 3$ and $\kappa = 13$ are used in the present study to calculate the laminar-sublayer thickness. The term τ_w/ρ is obtained by the Blasius relation:

$$\tau_w/\rho = 0.0396 Re^{-1/4} U_m{}^2 \tag{30}$$

where $Re = 2aU_m/v$ is the Reynolds number.

According to the continuity conditions, i.e. Eq. (28) and the boundary conditions, i.e. Eq. (20), the coefficients C_1~C_4 in Eq. (27) are obtained as:

$$\begin{cases} C_1 = \dfrac{C_3 I_0[(a-\delta)/\lambda_t]+\lambda C \sinh(\delta/\lambda)}{\cosh(\delta/\lambda)} \\ C_2 = -\lambda C \\ C_3 = \dfrac{\lambda^2 C}{\lambda \sinh(\delta/\lambda) I_0[(a-\delta)/\lambda_t]+\lambda_t I_1[(a-\delta)/\lambda_t]\cosh(\delta/\lambda)} \\ C_4 = 0 \end{cases} \tag{31}$$

2.2. Governing equations for the leak pipes

2.2.1 Equations of space charge density

With regard to a leak pipe, the flow field near the leak aperture is different from that of an intact pipe. In order to study the influence of leakage on the electrification of pipes, the velocity field **u**, see Eq. (10), near the leak is first investigated. In the present study, a computational fluid dynamics (CFD) numerical simulation is firstly performed on a two-dimensional model to simulate the flow field of a leak pipe. The length of the pipe is 2 m and the radius is 0.1 m. The radius of the leak aperture is 1/10 of the pipe radius. The *k*-*ε* model of Reynolds-Averaged Navier-Stokes's equations (RANS) is selected as the calculation model. Assuming that the whole pipe has formed a fully developed flow, whereas the average inlet velocity *U*m is set to 1 m/s, the simulation results show a little change of velocity near the leak aperture, see Fig. 3. Even so, the velocity change cannot be ignored. In this case, the charge conservation equation at the leak aperture is in the form of Eq. (10), while in other steady areas inside the pipe is in the form of Eq. (12).

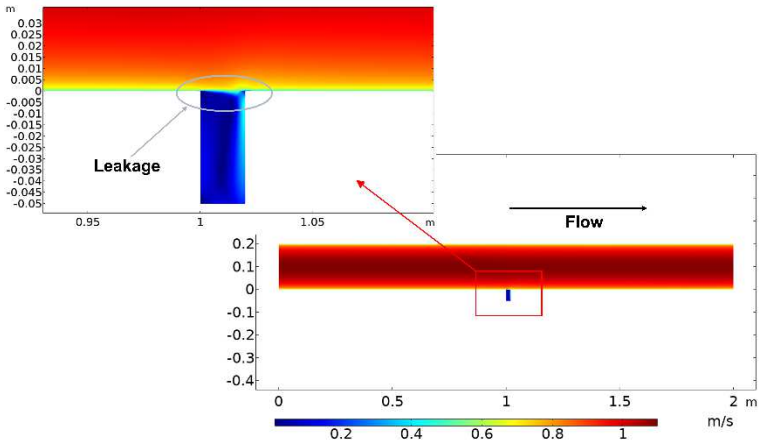

Fig.3. The flow filed near the leak aperture.

Existing literature report very few theoretical studies on the space charge density at the leak aperture of pipes. In order to obtain the governing equation for calculating the space charge

density at the leak aperture, the following assumptions are made in this study:

- (1) When the leakage reaches a steady state, the charge density at the leak aperture does not change with time ($\partial q/\partial t \approx 0$);
- (2) It is assumed that the diffusion term in Eq. (10) is negligible compared to the convection term and the conduction term at the leak aperture.

Therefore, Eq. (10) is simplified as:

$$\frac{\sigma q}{\varepsilon} + \nabla q \cdot \mathbf{u} = 0 \tag{32}$$

The radial flow at the leak aperture is dominant, while the axial flow can be neglected. Thus, the axial conduction is assumed as 0 ($u_x \partial q/\partial x = 0$) so that the conduction term $\nabla q \cdot \mathbf{u}$ is simplified as $u_r \partial q/\partial r$. Equation (32) is therefore derived as:

$$\frac{\sigma q_3}{\varepsilon} + u_r \frac{\partial q_3}{\partial r} = 0 \tag{33}$$

where u_r is the radial leak velocity; q_3 is the space charge density at the leak aperture.

2.2.2. Boundary conditions

It is noticed that Eq. (33) is a first-order differential equation. In order to solve Eq. (33), the initial boundary condition is needed. As shown in Fig. 4, here the charge density on the leakage aperture side of the leakage surface is assumed the same as that on the pipe inner side of the leakage surface, namely:

$$q_3\big|_{r=a} = q_1\big|_{r=a} = C_1 \tag{34}$$

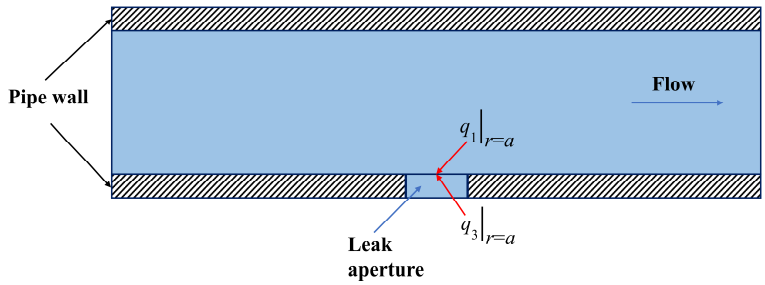

Fig.4. The diagram of the boundary condition of the space charge density at the leak aperture.

When the dielectric liquid leaks away from the surface, it follows the rules governed by Eq. (33).

2.2.3. Solutions to the space charge density

According to the governing equation in section 2.2.2 and the boundary condition in section 2.2.3, the solution to the space charge density at the leak aperture is:

$$q_3 = C_1 \exp(\frac{a}{u_r \tau}) \exp(-\frac{r}{u_r \tau}) \tag{35}$$

where $\tau = \varepsilon/\sigma$ is the relaxation time.

3. Simulations and results

3.1. Comparison of the proposed model and experimental data

The numerical simulations are performed on the commercial software COMSOL Multiphysics®, of which the Electrostatics interface is used to calculate the potential distributions in the pipe by solving the Poisson equation. In order to investigate the capacity of the proposed theoretical models of space charge density to estimate the electrostatic characteristics of intact and leak pipes, the case study is first compared with the experimental data reported by Zmarzly (2013). This case is carried out on a steel cylindrical pipe with the gasoline flowing. The reason for choosing gasoline is that it is a hazardous material and its vapor can easily form an explosive gas mixture with air (Qi et al., 2017). The gasoline vapor has a flashpoint of around −50 ℃ ~ −20 ℃ and its minimum ignition energy (MIE) is about 0.25 mJ. The explosive limit of gasoline vapor at mixture concentration is between 1.4% and 7.6% (Nabours, 2003). Due to its low MIE and low explosive limit, the gasoline vapor can be ignited by the electrostatic discharge, causing gasoline vapor explosions in the petrochemical industry. Table 1 shows the parameters related to the pipe and gasoline used in the case study. It is necessary to mention that these parameters refer to actual working conditions, technical manuals and scientific papers.

Table 1 The parameters of the pipe and gasoline.

Parameters	Values
Radius, a (m)	0.05
Length, L_1 (m)	0.7
Average velocity, U_m (m/s)	1.0
Density, ρ (kg/m^3)	720
Relative permittivity of gasoline, ε	1.9
Conductivity of gasoline, σ (S/m)	2.0×10^{-11}
Molecular diffusion coefficient, D_m (m^2/s)	1.0×10^{-9}
Kinematic viscosity of gasoline, v (m^2/s)	9.0×10^{-7}

The simplified three-dimensional pipe geometry for simulation is shown in Fig. 5. The constitutive material of the pipe is set as stainless steel and the wall thickness is 1/10 of the pipe diameter. According to the parameters of the pipe and gasoline, the Reynolds number of this flowing system is $1.1\times10^6 > 4000$, which indicates the turbulent flow inside the pipe. The shape of the velocity within a turbulent flow is well-established by both theory and experiments. In turbulent flow, the velocity in the laminar sublayer is approximately linear distribution, while in the turbulent zone the velocity is logarithmic. Thus, the axial velocity in turbulence is simplified as the average velocity U_m in the pipe cross-section. In the case study, the model is proposed under the premise that the pipeline has been fully developed. In order to reduce the simulation time, the inlet condition of the pipe section is set as the fully developed flow with the average velocity of 1 m/s and the pipe length of 0.7 m. The parameters A_t and n are set as

20 and 1, respectively (Wang and Meng, 2010). These values are adopted for the numerical simulation.

If the pipe is grounded, the accumulated charges on the external surface of the pipe will lead to leak current so that the charges will flow to the earth (Hou et al., 2017). Actually, it is proven that grounding the pipe wall to allow the charges accumulated on the wall to leak to the ground can effectively reduce the risk of explosion caused by the discharge (Astbury, 2008). Therefore, the wall boundary condition is defined as a fixed value of the electrostatic potential ($\phi = 0$).

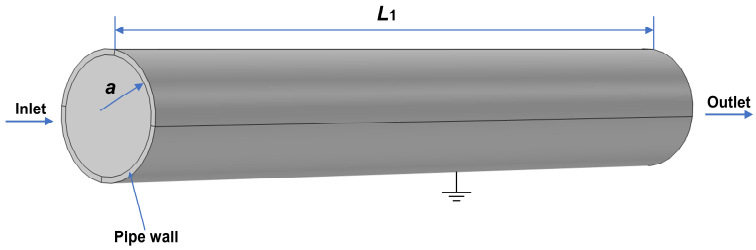

Fig.5. Schematic diagram of the three-dimensional intact pipe.

According to the Boltzmann distribution, 87% of diffuse layer charges are distributed between the compact layer (also called Stern sublayer), which is very close to the wall, and a distance from the wall equal to 2λ and 95% for 3λ (Paillat et al., 2001). This requires refined meshes near the wall for a good resolution in the laminar sublayer area. The step size in this region should be much smaller than the Debye length (Palmer and Nelson, 1997). In this study, the boundary layer mesh is used in the region very close to the pipe wall. The Debye length of the gasoline is 2.9×10^{-5} m and the smallest boundary layer thickness is 1×10^{-6} m so that the mesh is dense enough to achieve a good calculation accuracy in this region. In other regions far away from the wall, the refined free triangular mesh is used because it has advantages of good geometric strength, strong resistance to gross errors and high reliability.

The stationary solver is used to compute the static electricity of the pipe. Fig. 6 shows the space charge density distribution of the diameter of the pipe. The obtained results show that the charges are mostly distributed near the wall due to the mechanism of EDL, which also corresponds to the Boltzmann distribution. The space charge density decreases rapidly as the distance increases from the pipe wall.

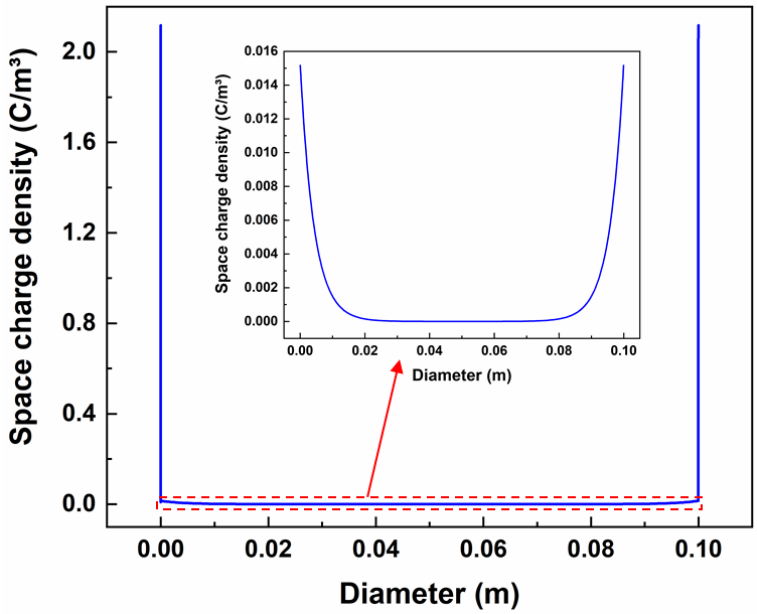

Fig.6. The space charge density distribution in the turbulent flow.

In order to evaluate the applicability of the proposed model, the simulation results shown in Fig. 6 are compared with the experimental data reported by Zmarzly (2013), which illustrated the impact of diffusion coefficient gradient on the charge density profile. If the diffusion change is small in the laminar sublayer, molecular diffusion plays an important role in the charge diffusion so that the charges are mainly distributed in the viscous layer. The diffusion coefficient in this study and the reported case is similar. The simulation results are compared with the reported experimental results, see Fig. 7. Figure 7 shows the logarithmic coordinates of the dimensionless charge density versus the logarithmic coordinate of dimensionless distance from the pipe wall. Since the parameters used in the simulations are not the same as the work done by Zmarzly, the sapce charge density distribution has a little differnce from his research, but the trends of the two curves are similar. The blue vertical line in Fig. 7 is the surface of the laminer sublayer and the turbulent zone. According to the parameters of the gasoline and the pipe, the laminar sublayer thickness δ is obtained as 4.8×10^{-5} m by solving Eq. (29). The dimensionless distance is 9.6×10^{-4}, the order of which is 10^{-3}, indicating that the laminar sublayer thickness is about 1/1000 of the pipe radius. Fig. 7 also shows that the charges are mainly distributed in the laminar sublayer, and the further away from the pipe wall, the faster the charge density decreases, which obeys the Boltzmann distribution. There is a maximum value of space charge density at the wall q_w, because the inner layer has the highest ion density and lowest ion mobility, while in the outer layer, the ion structure is less ordered and the ion mobility is higher (Qiao et al., 2008). The comparison in Fig. 7 shows that the charge distribution law obtained by the proposed model is very close to the experimental results, which demonstrates that the proposed model can be used to calculate the charge distribution in the pipe.

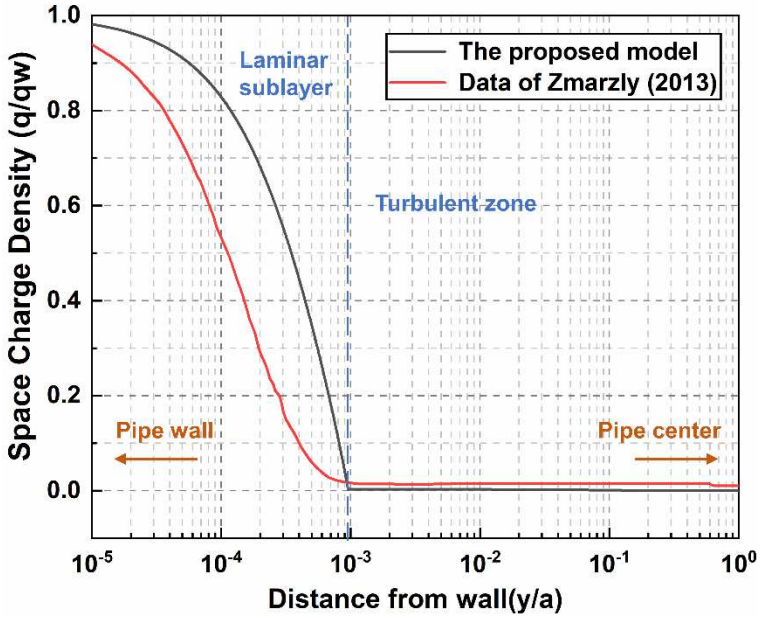

Fig.7. The space charge density versus the logarithmic distance from the wall.

The electrostatic potential is obtained by solving Poisson's equation, given in Eq. (11), and the calculated potential distribution along the radial direction is shown in Fig. 8. The electrostatic potential is distributed symmetrically along the central axis of the pipe. It also shows that the potential in the central area of the pipe is greater than that in the near-wall area. The maximum potential in the pipe is about 15 kV. The potential decreases from the central area to the pipe wall and the potential of the wall is 0 because the pipe wall is grounded. Although the potential is extremely high, the possibility of discharge is also associated with some other conditions, such as the electrical field strength, tip effect, etc.

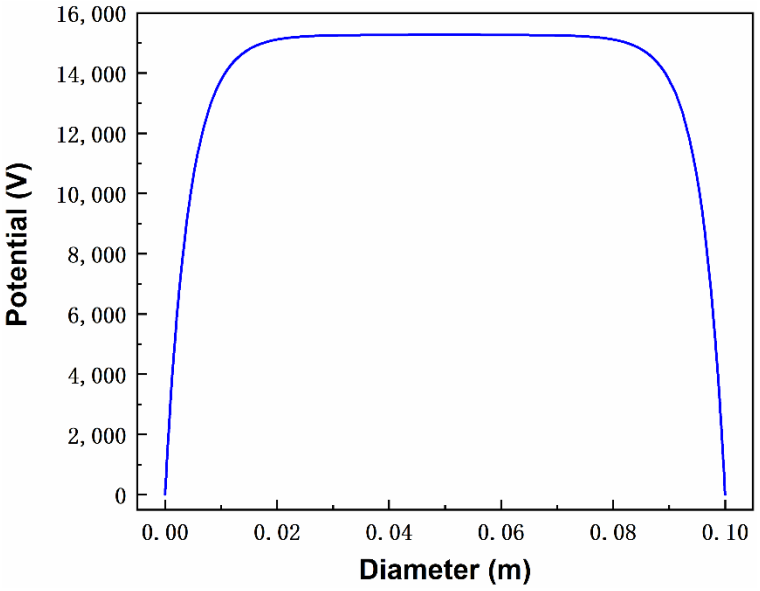

Fig. 8. The potential distribution along the radial direction.

3.2. The flow electrification of an intact pipe

3.2.1. The influence of the flow velocity

It is widely known that flow velocity has an impact on the electrification of dielectric liquid. The present paper investigates the influence of flow velocity on the charge density and electrostatic potential while other parameters of the pipe and the gasoline remaining constant. In order to prevent fire or explosion accidents caused by static electricity, when the conductivity of oil is less than 50 pS/m, the flow velocity of the inlet pipeline of light oil tank should be less than 4 m/s. Therefore, the velocities from 0.5 m/s to 4 m/s, with a step size of 0.5 m/s, are selected for simulation. Assuming that the conductivity of gasoline does not change with turbulent flow, the space charge densities under different velocities are shown in Fig. 9. Figure 9(a) shows the space charge density distributions of different flow velocities along the pipe section line through the diameter. In order to highlight the change of the space charge density at the pipe wall under different velocities, the charge distributions in logarithmic diameter are shown in Fig. 9(b). From Fig. 9 it can be seen that with the increase of flow velocity, the space charge densities at the pipe wall and in the laminar sublayer increase. The reason is that with the increase of velocity, the friction between liquid and pipe wall becomes more intense, which will generate more charges in the EDL.

On the other hand, the space charge density in the turbulent zone also increases with the increase of velocity. Larger velocity will also increase the turbulence intensity so that more charges are trapped into the turbulent zone from EDL, as shown in Fig. (10). The compact layer is close to the interface where the charges are not affected by the flow, but the charges in the diffuse layer can be flowed away (Dai et al., 2018).

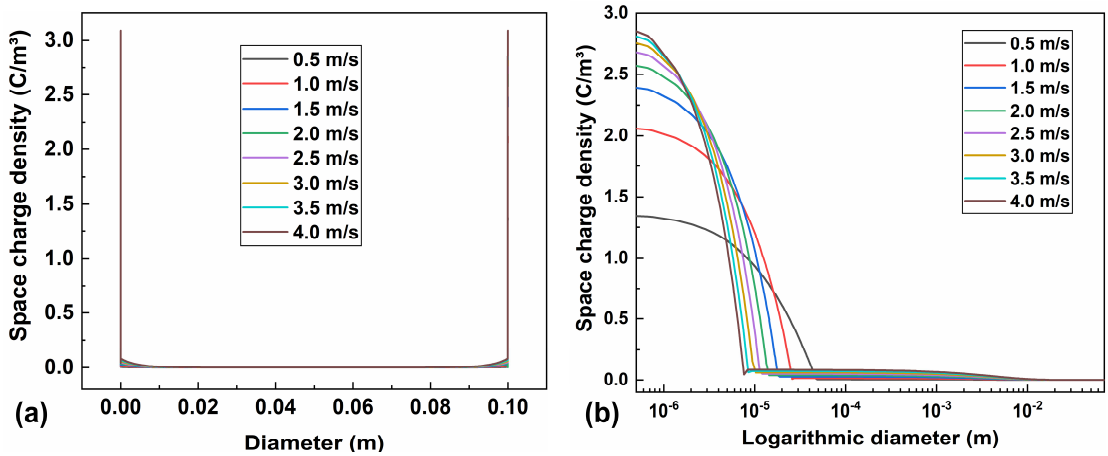

Fig.9. The space charge density distributions under different velocities: (a) space charge density distributions in both laminar sublayer and turbulence zone; (b) space charge density distributions along logarithmic diameter.

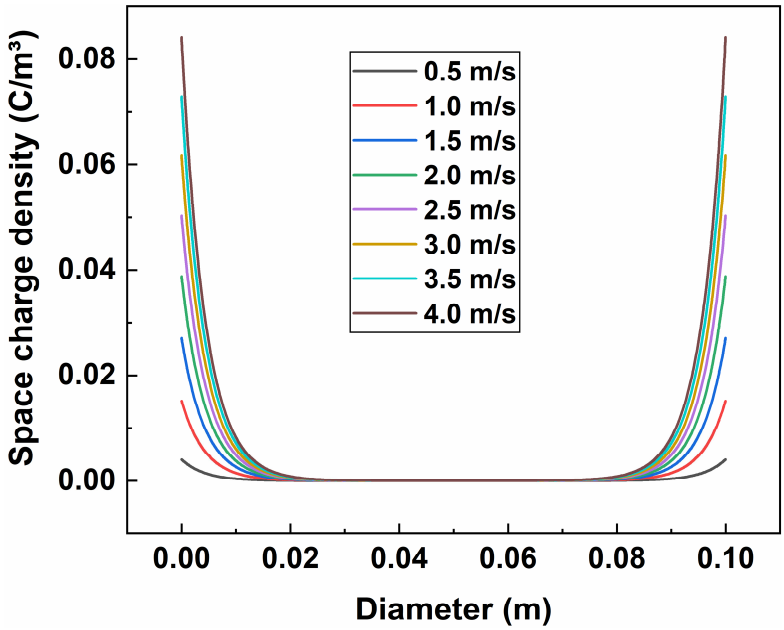

Fig.10. The space charge density distributions in the turbulent zone.

The electrostatic potential distributions of the pipe under different velocities are obtained using Poisson's equation, see Fig. 11(a). The peak value of the potential increases slowly with the increase of the flow velocity. In order to get the quantitative relationship between the maximum potential and the flow velocity, an exponential function is used to fit the maximum potential with respect to the velocity, as shown in Fig. 11(b). The fitted equation is $\phi = (20908\pm117) - (27259\pm960) \times (0.214\pm0.014)^{U_m}$. The correlation coefficient R-squared, in this case, equals 0.998, which indicates a small difference between the observed data and the fitted data.

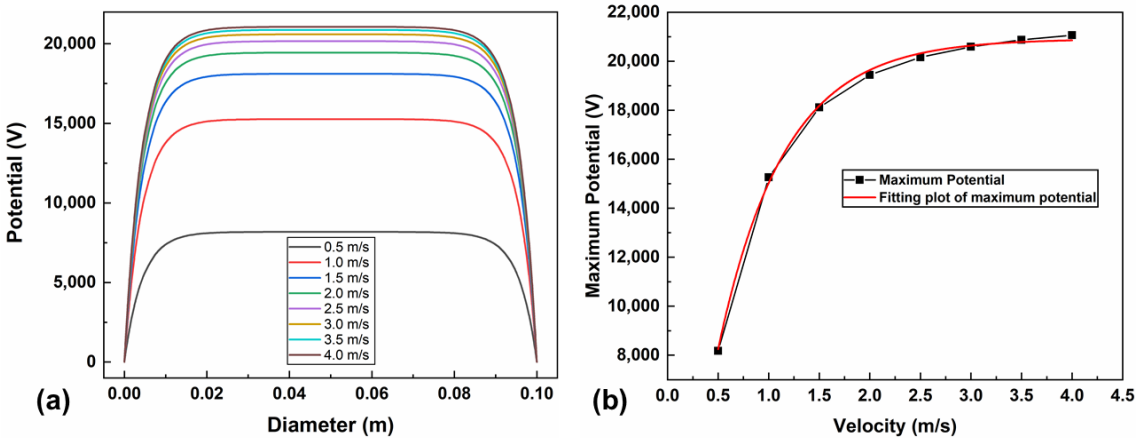

Fig. 11. The electrical potential distribution: (a) the distributions along the pipe diameter under different velocities; (b) the fitted curve of the maximum potential and flow velocity.

3.2.2. The influence of the pipe diameter

Different pipe diameters generate different space charge density, which may affect the safety of the pipe. Fig. 12 shows the distributions of the space charge density in the pipe under different diameters (D_i), whereas the other parameters of the pipe and the gasoline are kept constant, the flow velocity being set to 1 m/s. Fig. 12(a) shows that the space charge density in the laminar sublayer is greater than in the turbulent zone, under different pipe diameters. Meanwhile, the space charge density near pipe wall increases as the pipe diameters increase. On the contrary, Fig. 12(b) shows that the charge density at the interface between the turbulent zone and the laminar sublayer decreases with the growth of the pipe diameters.

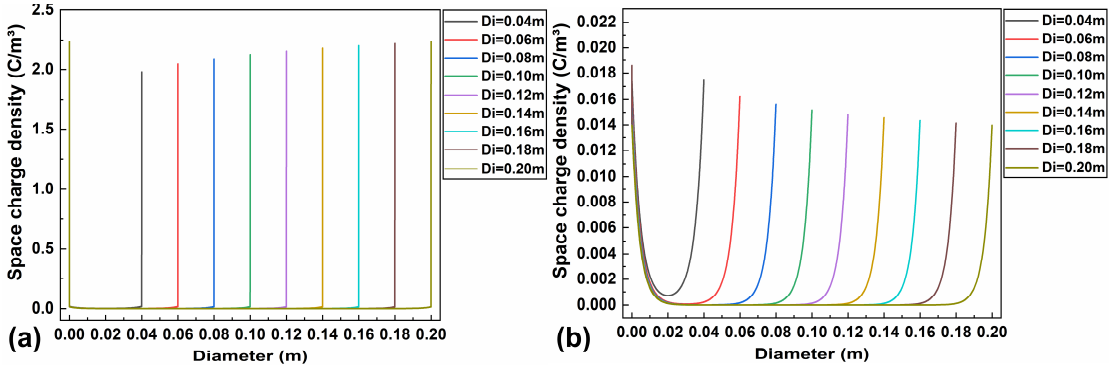

Fig. 12. The space charge density distribution under different pipe diameters: (a) the charge density in laminar sublayer and turbulent zone; (b) the detailed charge density in the turbulent zone.

Moreover, the distributions of the electrostatic potential of the pipe under different diameters are also simulated. The results, see Fig. 13(a), show that the maximum potential decreases as the pipe diameter increases. The quantitative relationship between the maximum potentials and the pipe diameters is fitted using an exponential function, and the fitted curve is shown in Fig. 13(b). The fitted equation is $\phi = (13381\pm96) + (5181\pm60) \times \exp[-r/(0.1\pm0.006)]$, with an R-squared equal to 0.999, indicating that this fitted equation can be used to predict the relationship between the maximum potential and the pipe diameter.

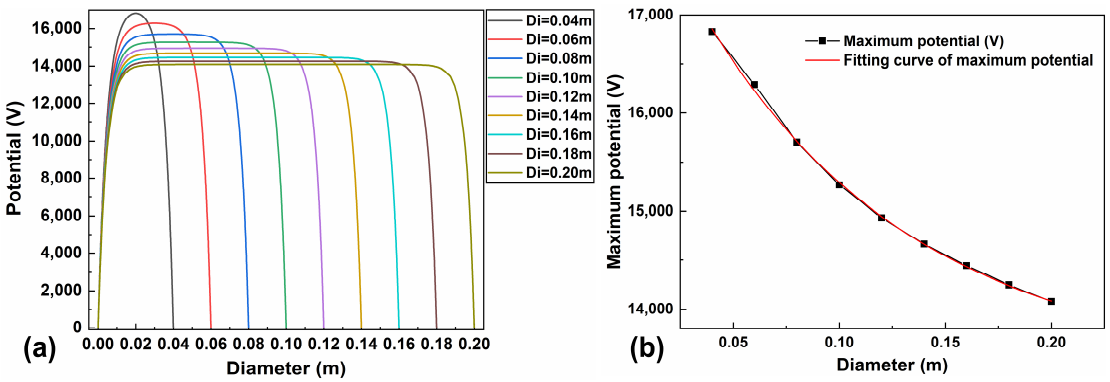

Fig. 13. The electrical potential distributions: (a) the distributions along the pipe diameter under different diameters; (b) the fitted curve of the maximum potential and pipe diameters.

3.3. The flow electrification of a leak pipe

From above analysis, it is clear that in turbulent flow, a large number of static charges are accumulated due to the friction when the dielectric liquid flows in the pipe, which will generate electrostatic potential. If an accident occurs, for instance, the pipe is not well grounded, it may cause electrostatic discharge. When there is flammable gas and its concentration reaches the flammability limit, fire or explosion accidents may occur. Unfortunately, pipe leakage increases the probability of flammable gas in the ambient environment. Therefore, it is of great importance to investigate the influence of the pipe leakage on the space charge density distribution and potential distribution.

3.3.1. The influence of the flow velocity

The present paper also investigates the electrostatic characteristics of the leak pipe. Numerical simulations are run to study the distributions of space charge density and electrostatic potential, which are used to characterize the electrostatic hazard of the leak pipe. The flowing fluid is also gasoline, and the explosion limit of gasoline vapor is about 1% ~ 6%. In other words, when the concentration of the leaked gasoline vapor exceeds 1%, and in the presence of an ignition source such as the electrostatic spark, a fire or explosion accident may occur. The basic parameters for numerical simulations of the leak pipe are the same than in Table 1 except for the leak aperture. The leak aperture has a simple form, i.e., a circular hole and the radius of it is 1/10 of the pipe radius, as shown in Fig. 14. The leak aperture is located in the middle of the pipe.

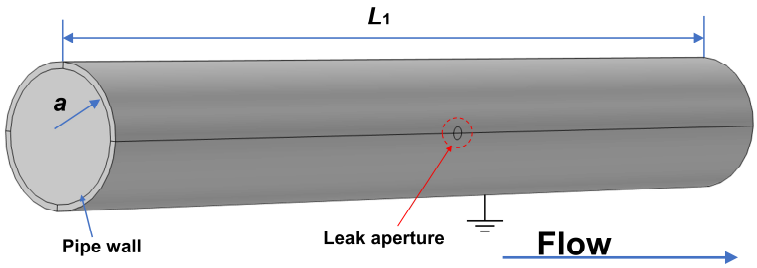

Fig. 14. Schematic diagram of the three-dimensional leak pipe.

The simulations of the space charge density distributions of the leak pipe under different velocities are conducted. The charge density under the velocity of 1 m/s of the pipe section line through the leak aperture is selected as an example to illustrate. As shown in Fig. 15, the abscissa 0-0.1 represents the range I i.e., inside the pipe, while the abscissa 0.1-0.105 represents the range II i.e., leak aperture. The distribution of space charge density inside the pipe (range I) is symmetrical, which is the same as that of the intact pipe. However, at the leakage aperture (range II) of the pipeline, the charge density of the leakage liquid decreases with the increase of the outflow distance. In order to see the influence of flow velocity on the space charge density distribution, the curves of space charge density under different velocities are put together, as

shown in Fig. 16. The space charge density at the leak aperture increases with the increase of the flow velocity, but the increase rate slows down.

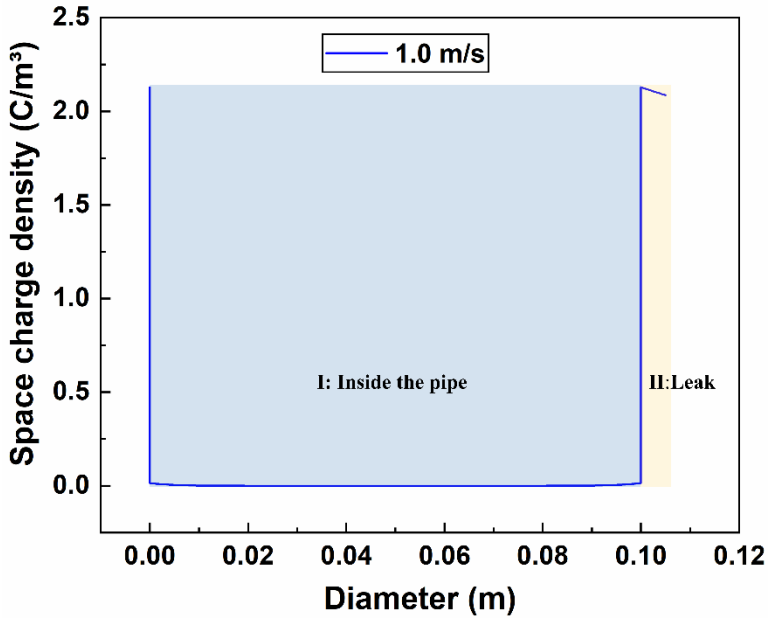

Fig. 15. Space charge density distribution of leak pipe under the velocity of 1 m/s.

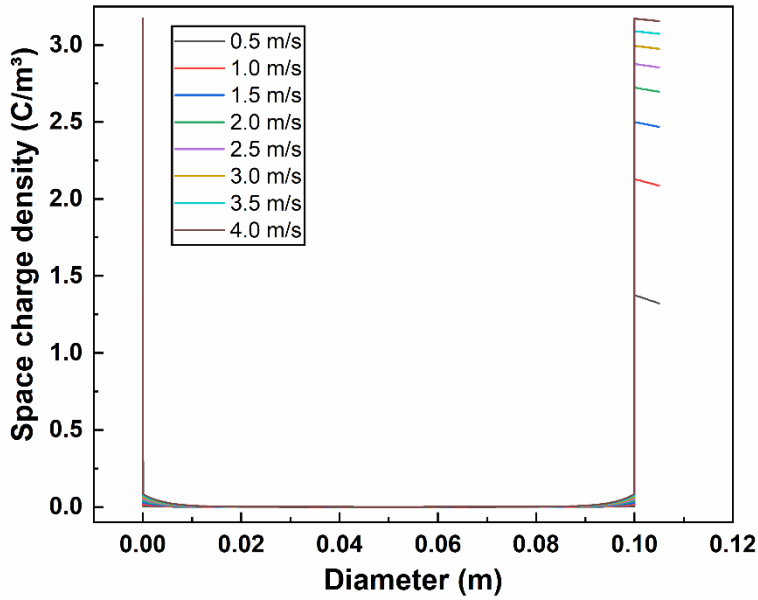

Fig. 16. The space charge density distribution along the diameter line passing through the leak aperture under different velocities.

The simulations of the electrostatic potential distributions of the leak pipe under different velocities are also conducted. Figure 17 shows the two-dimensional potential distribution on the radial section carried by the plane including the leak aperture at the flow velocity of 1 m/s. The potential distribution is different from that of an intact pipe. The maximum potential of the leak pipe appears at the leak aperture, while the maximum potential of the intact pipe appears in the central area of the pipeline.

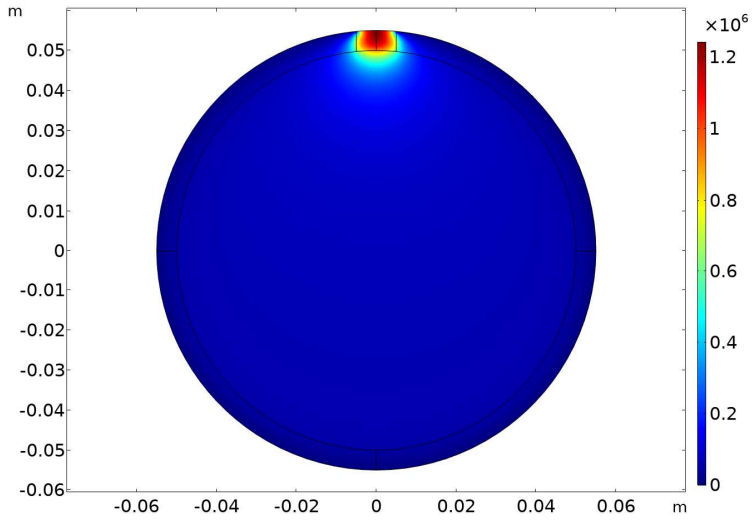

Fig. 17. The potential distribution on the radial section carried by the plane including the liquid leakage aperture.

In order to show the changes of the potential, the distributions along the diameter line passing through the leak aperture under different velocities are investigated, as shown in Fig. 18(a). Range I shows the potential inside the pipe while range II shows the potential at the leak aperture. Different from intact pipes, the potential distributions in range I of leak pipes are asymmetric and the internal potential of the pipe near the leak aperture increases rapidly. The potential increases gradually with the distance from the leak surface and it can reach more than several megavolts. Meanwhile, the potential at the leak increases with the increase of the flow velocity in the pipe, and the increase rate slows down.

In order to get the quantitative relationship between the maximum potential of leak pipes and the flow velocity, an exponential function fits the maximum potential with respect to the velocity, as shown in Fig. 18(b). The fitted equation is $\phi = (196043 \pm 33579) - (175791 \pm 64283) \times \exp[-U_m/(1.19 \pm 0.10)]$, with an R-squared equal to 0.994.

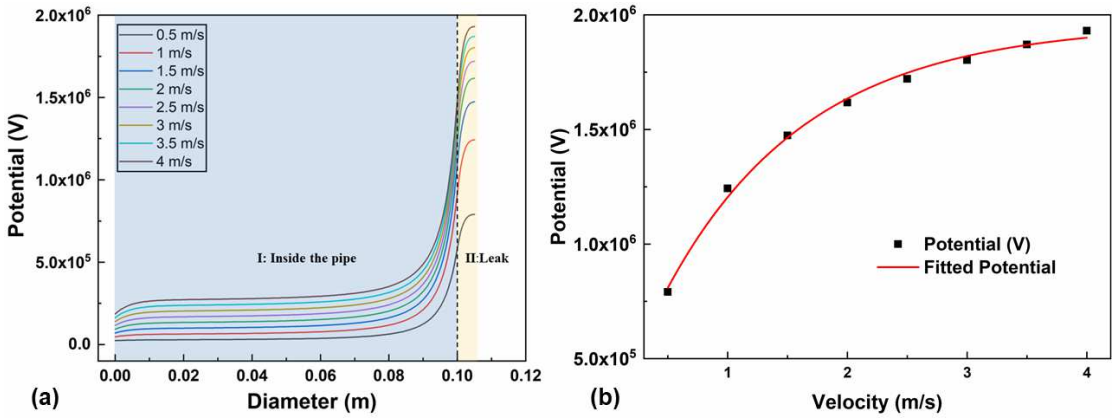

Fig. 18. The potential distributions in leak pipes under different velocities: (a) the distributions along the diameter line passing through the leak aperture; (b) the curve of the maximum potential versus flow velocity.

3.3.2. The influence of the pipe diameter

The influence of the pipe diameter on the electrostatic characteristics of the leak pipe is also conducted. The velocity is also set to 1 m/s and other parameters are detailed in Section 3.3. The pipe wall thickness is 1/10 of the pipe radius. The space charge density distributions along the diameter line passing through the leak aperture is simulated. The results, see Fig. 19(a), show that the maximum space charge density appears near the wall, which is consistent with the distribution law of intact pipes. The maximum space charge density increases as the pipe diameter increases. Meanwhile, the space charge density at the leak aperture decreases linearly with the distance from the leak surface.

Figure 19(b) shows the potential distributions along the diameter line passing through the leak aperture under different diameters. It confirms again that the maximum potential appears at the leakage outlet. The maximum potential at the leak aperture increases with the increase of pipe diameter. In other words, the risk of electrostatic discharge of leak pipes is higher when the pipe diameter is larger.

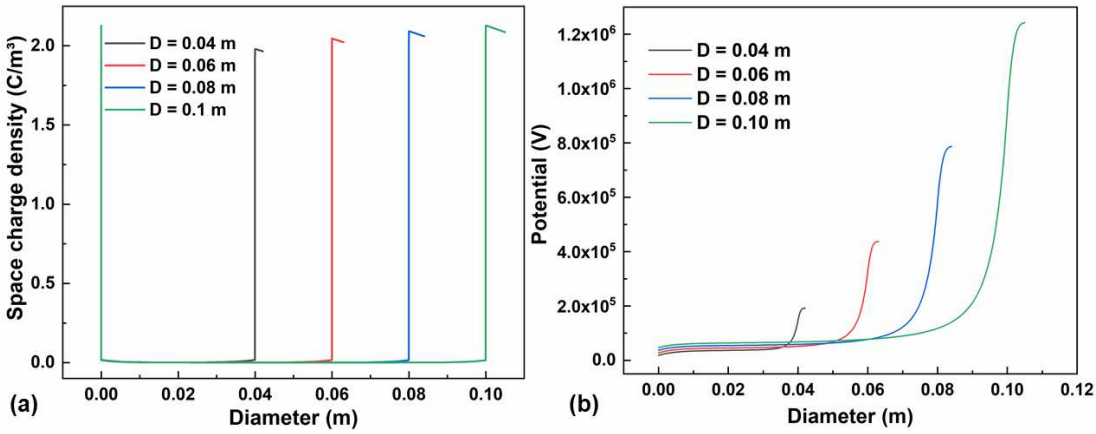

Fig. 19. The distributions along the diameter line passing through leak aperture under different pipe diameters: (a) the space charge density distributions; (b) The potential distributions.

4. Discussion

Fire and explosion caused by electrostatic discharge shall meet the following conditions at the same time: 1) electrostatic charges are accumulated to a threshold of potential and/or field strength sufficient to cause discharge; 2) combustible or explosive vapor mixture around electrostatic discharge; 3) the energy produced by electrostatic discharge should reach the MIE of the combustible mixture. There are several types of electrostatic discharge, such as the spark discharge, the brush discharge, which are the most dangerous discharge types in industrials.

Since the presence of sufficiently high electrostatic potentials and/or electrostatic discharges are the two key issues for electrostatic ignition (Hearn et al., 2012), this paper takes the electrostatic potential as an index to measure the electrostatic risk of the pipeline. The electrostatic potentials developed on the walls of the piping during fuel flow were all significantly below the 20 kV threshold for brush discharges to occur (Hearn, 2002). Although the energy released by brush discharge is less than that of spark discharge, it is still possible to ignite gasoline vapor. Therefore, the potential of 20 kV is selected as the threshold to analyze the electrostatic hazard.

The flow electrification of intact and leak pipes is studied in Sections 3.2 and 3.3, respectively. For both intact and leak pipes, the maximum potentials increase with the increase of flow velocity and pipe diameter. As shown in Fig. 11 of the intact pipe, when the flow velocity in the pipe exceeds 2.5 m/s, the maximum potential exceeds the threshold value of 20 kV, thus the velocities exceeding 2.5 m/s are seen as the dangerous velocities that may cause electrostatic discharge. However, as for the leak pipe, see Fig. 18, the potential distributions of different velocities are different from that of the intact pipe. The maximum potential appears at the leak aperture and also increases with the increase of the flow velocities. The maximum potential under each velocity of the leak pipe can be up to several megavolts, which exceeds the threshold value. Therefore, the electrostatic hazard of leak pipes is higher than the intact pipes.

When a pipe leaks, not only does the electrostatic potential increase significantly, but also the leaked gasoline may volatilize and form a flammable atmosphere. Even if the potential of leak pipe is very high, it still needs to meet the conditions for electrostatic discharge to occur, such as spark discharge or brush discharge. A spark discharge normally occurs between two conductive parts, at least one of which is not grounded, while a brush discharge normally occurs between a charged exposed insulating surface and a conductive electrode (Merilo et al., 2012). The theoretical models and the simulation method proposed in this research are capable of evaluating the electrostatic hazard of intact and leak pipes based on the potential. According to the analysis in this research, in order to reduce the possibility of electrostatic discharge, the flow velocity ought to be controlled below 2.5 m/s, and the pipes with smaller diameter shall be used as far as possible when meeting the requirement for use.

5. Conclusion

This paper deals with the flow electrification of turbulent flow both in intact and leak pipes. It focuses on the space charge density which is a key issue for the analysis on the flow electrification in pipes. The theoretical models proposed to calculating the space charge density of intact and leak pipes are based on the charge conservation equation.

The study assumes a set of spatial boundary conditions, requested to solve the differential equations, based on the discharge mechanism.

The theoretical model is interfaced with COMSOL Multiphysics software to simulate the electrostatic potential. The simulated space charge density is in accordance with the experimental data, and shows that the charges are mainly distributed in laminar sublayer, and the further away from the pipe wall, the faster the charge density decreases.

The study of the effects of both flow velocity and pipe radius, on the electrostatic characteristics in intact and leak pipes are studied shows that

- *For the intact pipes*: The electrostatic potential decreases from the central area to the pipe wall. The maximum potential increases slowly with the increase of the flow velocity. The quantitative relationship between the maximum potential and the mean flow velocity can be expressed by an exponential function. As well, the maximum potential decreases with the increase of the pipe radius and the quantitative relationship between the maximum potential and the pipe radius can be also expressed by an exponential function.
- *For the leak pipes*: The leak aperture influences the flow field, thereby affecting the potential distributions. The potential distribution in the leak pipe is asymmetrically distributed with the central axis of the pipe. The maximum potential appears at the leak aperture, and increases with the increase of flow velocity and pipe radius. The potential of 20 kV is selected as the threshold to analyze the electrostatic hazard. On this basis, the flow velocity below 2.5 m/s and a small diameter are regarded as safe conditions.

Acknowledgements

The authors thank the support given by the National Natural Science Foundation of China (51834007). The first author is also grateful for the support of the "Postgraduate Research & Practice Innovation Program of Jiangsu Province (KYCX20_1036)" and the "Cultivation Program for The Excellent Doctoral Dissertation of Nanjing Tech University".

Notation

Symbol	Explanation	Unit
A_t	a constant determined by experimental data	
a	pipe radius	m
b	$b= r/\lambda_t$	
C_1~C_4	coefficients that need to be determined using boundary conditions	
C_{-o}	concentration of the negative ions in the liquid bulk	mol/m^3
C_s	concentration of the negative ions at the surface	mol/m^3
D	diffusion coefficient	m^2/s
D_m	molecular diffusion coefficient	m^2/s
D_t	turbulent diffusion coefficient	m^2/s
d	diffuse layer thickness	m
$\mathbf{E}$	electric field	V/m
$\overline{E}$	average electric field near the wall	V/m

e_0	electrical charge of a particle	C
F	Faraday's constant	C/mol
$I_0()$	zero-order modified Bessel functions of the first kind	
$\mathbf{j}$	current density	A/m^2
j_s	streaming current at the surface	A
j_w	streaming current	A
k	Boltzmann constant	J/K
$K_0()$	zero-order modified Bessel functions of the second kind	
L	length of an infinite pipe	m
L_1	length of the studied pipe section	m
m	empirical coefficient	
n	a constant determined by experimental data	
n_+	transference number of the positive ions	
q	space charge density	C/m^3
q_1	charge density in laminar sublayer	C/m^3
q_2	charge density in turbulent region	C/m^3
q_3	space charge density at the leak aperture	C/m^3
Re	Reynolds number	
r	pipe radius	m
S	Schmidt number	
T	absolute temperature	K
t	time	s
$\mathbf{u}$	velocity field	m/s
U_m	average velocity in the pipe cross-section	m/s
u_r	radial leak velocity	m/s
$\bar{u}_x$	time-averaged axial velocity	m/s
y	disntance from pipe wall	m
δ	thickness of the laminar sublayer	m
ε	relative permittivity	F/m
ε_0	vacuum permittivity	F/m
ε_r	relative permittivity	
κ	empirical coefficient	
λ	Debye length	m
λ_t	turbulent Debye length	m
μ	average mobility of the positive and negative ions	$cm^2/(V \cdot s)$
ν	kinematic viscosity of the liquid	m^2/s
ρ	liquid density	kg/m^3
σ	liquid conductivity	S/m
τ	relaxation time	s
τ_w	shear stress at the wall	Kg/m^2
ϕ	electrical potential	V

Reference

Abedian, B., Sonin, A.A., 1986. Electric currents generated by turbulent flows of liquid hydrocarbons in smooth pipes: Experiment vs. theory. Chem. Eng. Sci. 41, 3183–3189. https://doi.org/10.1016/0009-2509(86)85055-2

Abedian, B., Sonin, A.A., 1982. Theory for electric charging in turbulent pipe flow. J. Fluid Mech. 120, 199–217. https://doi.org/10.1017/S0022112082002730

Astbury, G.R., 2008. A review of the properties and hazards of some alternative fuels. Process Saf. Environ. Prot. 86, 397–414. https://doi.org/10.1016/j.psep.2008.05.001

Boumans, A.A., 1957. Streaming currents in turbulent flows and metal capillaries. Physica 23, 1047–1055. https://doi.org/10.1016/s0031-8914(57)96078-0

Chou, H.C., Yeh, C.T., Shu, C.M., 2015. Fire accident investigation of an explosion caused by static electricity in a propylene plant. Process Saf. Environ. Prot. 97, 116–121. https://doi.org/10.1016/j.psep.2015.02.007

COMSOL Multiphysics® v. 5.4. cn.comsol.com. COMSOL AB, Stockholm, Sweden. 2018

Dai, J., Wu, K., Cheng, C., 2018. Effects of space charge on flow electrification characteristics under DC voltage. IEEE Trans. Dielectr. Electr. Insul. 25, 1492–1501. https://doi.org/10.1109/TDEI.2018.006977

El-Adawy, M., Paillat, T., Touchard, G., Cabaleiro, J.M., 2011. Numerical simulation of the electrical double layer development: Physicochemical model at the solid and dielectric liquid interface for laminar flow electrification phenomenon. IEEE Trans. Dielectr. Electr. Insul. 18, 1463–1475. https://doi.org/10.1109/TDEI.2011.6032817

Gavis, J., 1964. Transport of electric charge in low dielectric constant fluids. Chem. Eng. Sci. 19, 237–252. https://doi.org/10.1016/0009-2509(64)85034-X

Gavis, J., Koszman, I., 1961. Development of charge in low conductivity liquids flowing past surfaces: A theory of the phenomenon in tubes. J. Colloid Sci. 16, 375–391. https://doi.org/10.1016/0095-8522(61)90036-8

Giles, M.R., 2003. Electrostatic Hazards in Liquids and Relevance to Process Chemistry. Org. Process Res. Dev. 7, 1048–1050. https://doi.org/10.1021/op0340863

Hearn, G.L., 2002. Electrostatic ignition hazards arising from fuel flow in plastic pipelines. J. Loss Prev. Process Ind. 15, 105–109. https://doi.org/10.1016/S0950-4230(01)00061-4

Hearn, G.L., von Pidoll, U., Smallwood, J.M., Ticci, A., 2012. An assessment of electrostatic ignition hazards associated with fuel flow through plastic pipes at roadside filling stations. J. Electrostat. 70, 179–183. https://doi.org/10.1016/j.elstat.2011.11.002

Hou, X.H., Yu, J.K., Sheng, M.K., Liu, Z.Y., Yang, X., 2017. Influence factors of the generation and accumulation of electric charge on the oil-delivery metal pipelines. Acta Metall. Sin. (English Lett. 30, 1027–1032. https://doi.org/10.1007/s40195-017-0623-2

Huang, B., Hao, M., Hao, J., Fu, J., Wang, Q., Chen, G., 2016. Space charge characteristics in oil and oil-impregnated pressboard and electric field distortion after polarity reversal. IEEE Trans. Dielectr. Electr. Insul. 23, 881–891. https://doi.org/10.1109/TDEI.2015.005413

Koszman, I., Gavis, J., 1962. Development of charge in low-conductivity liquids flowing past surfaces. Chem. Eng. Sci. 17, 1023–1040. https://doi.org/10.1016/0009-2509(62)80081-

5
Leblanc, P., Cabaleiro, J.M., Paillat, T., Touchard, G., 2017. Impact of the laminar flow on the electrical double layer development. J. Electrostat. 88, 76–80. https://doi.org/10.1016/j.elstat.2016.11.006
Merilo, E.G., Groethe, M.A., Adamo, R.C., Schefer, R.W., Houf, W.G., Dedrick, D.E., 2012. Self-ignition of hydrogen releases through electrostatic discharge induced by entrained particulates. Int. J. Hydrogen Energy 37, 17561–17570. https://doi.org/10.1016/j.ijhydene.2012.03.167
Moreau, E., Paillat, T., Touchard, G., 2001. Space charge density in dieletric and conductive liquids flowing through a glass pipe. J. Electrostat. 51–52, 448–454. https://doi.org/10.1016/S0304-3886(01)00082-1
Nabours, R.E., 2003. Static discharge hazard in explosive atmospheres. IEEE Tech. Conf. Ind. Commer. Power Syst. 2003 66–68. https://doi.org/10.1109/icps.2003.1201489
Nelson, J.K., Brubaker, M.A., Palmer, J.A., 2003. The Formulation of Models for the Description of Streaming Electrification in Transformer Structures. IEEE Trans. Dielectr. Electr. Insul. 10, 920–932. https://doi.org/10.1109/TDEI.2003.1255768
Ohsawa, A., 2011. Statistical analysis of fires and explosions attributed to static electricity over the last 50 years in Japanese industry. J. Phys. Conf. Ser. 301. https://doi.org/10.1088/1742-6596/301/1/012033
Paillat, T., Moreau, E., Touchard, G., 2001. Space charge density at the wall in the case of heptane flowing through an insulating pipe. J. Electrostat. 53, 171–182. https://doi.org/10.1016/S0304-3886(01)00139-5
Palmer, J.A., Nelson, J.K., 1997. The simulation of short-term streaming electrification dynamics. J. Phys. D Appl. Phys. 30, 1207–1213.
Pavey, I.D., 2004. Electrostatic hazards in the process industries. Process Saf. Environ. Prot. 82, 132–141. https://doi.org/10.1205/095758204322972771
Qi, S., Du, Y., Zhang, P., Li, G., Zhou, Y., Wang, B., 2017. Effects of concentration, temperature, humidity, and nitrogen inert dilution on the gasoline vapor explosion. J. Hazard. Mater. 323, 593–601. https://doi.org/10.1016/j.jhazmat.2016.06.040
Qiao, Y., Han, A., Punyamurtula, V.K., 2008. Electrification of a nanoporous electrode in a continuous flow. J. Phys. D. Appl. Phys. 41. https://doi.org/10.1088/0022-3727/41/8/085505
Touchard, G., 1978. Streaming currents developed in laminar and turbulent flows through a pipe. J. Electrostat. 5, 463–476. https://doi.org/10.1016/0304-3886(78)90038-4
Touchard, G., Patzek., T., Radke, C., 1996. A physicochemical explanation for flow electrification in low-conductivity liquids in contact with a corroding wall. IEEE Trans. Ind. Appl. 32, 1051–1057. https://doi.org/10.1109/28.536865
Walmsley, H.L., 2012. Electrostatic ignition hazards with plastic pipes at petrol stations. J. Loss Prev. Process Ind. 25, 263–273. https://doi.org/10.1016/j.jlp.2011.11.002
Wang, J. F., Meng, H. L., 2009. Computation of streaming current in oil pipes. IEEE Trans. Dielectr. Electr. Insul. 16, 299–304. https://doi.org/10.1109/TDEI.2009.4815156
Wang, J.F., Meng, H.L., 2010. Calculation of oil flow electrification current in pipeline. J. China Univ. Pet. (Edition Nat. Sci.) 34, 131–135. https://doi.org/10.3969/j.issn.1673-5005.2010.05.024

Zdanowski, M., 2020. Streaming Electrification Phenomenon of Electrical Insulating Oils for Power Transformers. Energies 13, 3225. https://doi.org/10.3390/en13123225

Zheng, W., Hu, Y., Liu, C., Wei, X., Hao, L., 2013. The simulation of electrostatics elimination effect influenced by the cross-section shape of discharge needles, in: Journal of Physics: Conference Series. https://doi.org/10.1088/1742-6596/418/1/012017

Zhu, Y., Qian, X.M., Liu, Z.Y., Huang, P., Yuan, M.Q., 2015. Analysis and assessment of the Qingdao crude oil vapor explosion accident: Lessons learnt. J. Loss Prev. Process Ind. 33, 289–303. https://doi.org/10.1016/j.jlp.2015.01.004

Zmarzly, D., 2013. Streaming electrification current model in a round pipe in turbulent regime. IEEE Trans. Dielectr. Electr. Insul. 20, 1497–1509. https://doi.org/10.1109/TDEI.2013.6633676